

Thermal decomposition of dinuclear complexes $\text{LM}(\mu\text{-OOCR})_4\text{ML}$ (L is α -substituted pyridine).

1. Synthesis, structures, and solid-state thermolysis of Mn^{II} , Fe^{II} , Co^{II} , Ni^{II} , and Cu^{II} pivalates with apical 2,3-dimethylpyridine and quinoline ligands

I. G. Fomina,^{a*} Zh. V. Dobrokhotova,^a M. A. Kiskin,^a G. G. Aleksandrov,^a O. Yu. Proshenkina,^a A. L. Emelina,^b
V. N. Ikorskii,^{c†} V. M. Novotortsev,^a and I. L. Eremenko^a

^aN. S. Kurnakov Institute of General and Inorganic Chemistry, Russian Academy of Sciences,
31 Leninsky prosp., 119991 Moscow, Russian Federation.

Fax: +7 (495) 954 1279. E-mail: fomina@igic.ras.ru

^bDepartment of Chemistry, M. V. Lomonosov Moscow State University,
1 Leninskie Gory, 119992 Moscow, Russian Federation.

E-mail: emelina@td.chem.msu.ru

^cInternational Tomography Center, Siberian Branch of the Russian Academy of Sciences,
3a ul. Institutskaya, 630090 Novosibirsk, Russian Federation

Fax: +7 (383 2) 33 1399. E-mail: ikorsk@tomo.nsc.ru

The solid-state thermal decomposition of the tetrabridged dinuclear Mn^{II} , Fe^{II} , Co^{II} , Ni^{II} , and Cu^{II} pivalate complexes with apical α -substituted pyridine ligands containing different substituents (2,3-dimethylpyridine or quinoline) was studied by differential scanning calorimetry and thermogravimetry. The decomposition of the Co^{II} complexes is accompanied by the aggregation to form the volatile octanuclear complex $\text{Co}_8(\mu_4\text{-O})_2(\mu_n\text{-OOCMe}_3)_{12}$, where $n = 2$ or 3, whereas the thermolysis of the Mn^{II} , Fe^{II} , Ni^{II} , and Cu^{II} complexes is accompanied by the degradation of the starting compounds, the phase composition of the decomposition products being substantially dependent on the nature of metal and the apical organic ligand.

Key words: dinuclear tetrabridged manganese, iron, cobalt, nickel, and copper pivalate complexes, 2,3-dimethylpyridine, quinoline, solid-state thermal decomposition, X-ray diffraction study, magnetic properties.

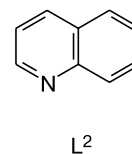
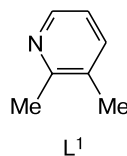
Dinuclear complexes of Group VII and VIII 3d transition metals with four bridging pivalate ligands $\text{LM}(\mu\text{-OOCR})_4\text{ML}$ are readily soluble in organic solvents. Among these compounds, the Co^{II} ,^{1–3} Ni^{II} ,^{4,5} Fe^{II} , and Mn^{II} (see Ref. 6) complexes have received the most study. These compounds have attracted attention as convenient models for studying the magnetic behavior of systems containing two high-spin centers.^{7–9} The relative ease of their synthesis gives hope that these compounds can find wider application. In particular, these complexes, including copper derivatives, are of interest for the preparation of various coatings. To predict the prospects of the application of such dinuclear systems in the formation of films or nanosized coatings, it is important to study the thermal decomposition steps and determine the character of thermolysis products. Their composition often depends on the nature of precursors, in particular, on the nature of the organic moiety in the starting complex molecules, because the latter has a considerable effect on intra-

molecular redox reactions involved in the thermolysis of the complexes.

In the present study, we synthesized dinuclear tetrabridged Mn, Fe, Co, Ni, and Cu pivalate complexes with α -substituted pyridines containing different substituents, viz., 2,3-dimethylpyridine ($2,3\text{-(CH}_3)_2\text{C}_5\text{H}_3\text{N}$) and quinoline ($\text{C}_9\text{H}_7\text{N}$), as the apical ligands L and studied the thermolysis of these complexes.

Results and Discussion

The main synthetic goal of the present study was to prepare dinuclear pivalate complexes with apically coordinated substituents of different nature.



[†] Deceased.

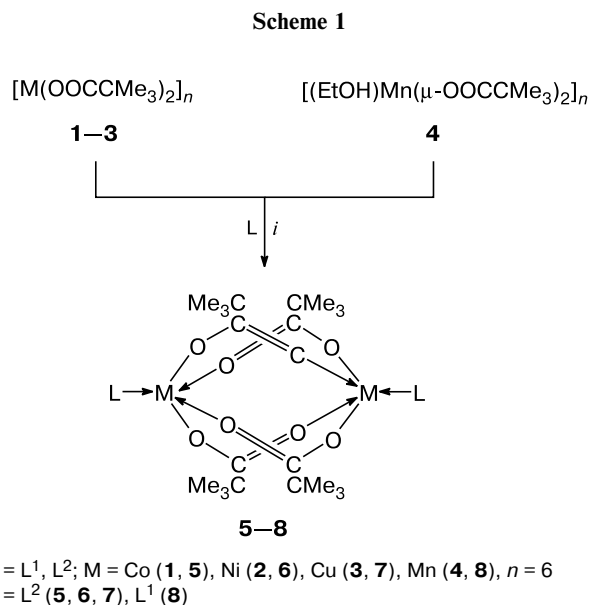
We expected that in the ligands used in the present study (L^1 is 2,3-dimethylpyridine and L^2 is quinoline), the protons of the Me groups in the α position of the ligand L^1 would be most active with respect to the metal carboxylate core due to their geometric arrangement in the dinuclear complexes and could formally interact with the oxygen atoms of the carboxylate bridges. Unlike these protons, the proton in the α position of the ligand L^2 is substantially more distant (~ 2 Å) from the oxygen atoms of the pivalate bridges and is unlikely to interact with this fragment.

1. Synthesis of dinuclear Mn, Co, Ni, and Cu pivalates

Although some $LM(\mu\text{-OOCBu}^t)_4ML$ complexes of the series under consideration ($L = L^1$; $M = \text{Co}$ ³ or Ni ^{3,4}; $L = L^2$, $M = \text{Co}$ ¹; L is 2-methylquinoline, $M = \text{Ni}$ ⁵) have been characterized, and the procedures for their synthesis have been documented, we supplemented the scope of these compounds. The directed degradation of the $[M(\text{OOCBu}^t)_2]_n$ ($M = \text{Co}$ (1), Ni (2), or Cu (3)) or $[(\text{EtOH})\text{Mn}(\mu\text{-OOCMe}_3)_2]_n$ (4) polymers in benzene with 2,3-dimethylpyridine (L^1) or quinoline (L^2) was used as the main procedure for the synthesis of new complexes (Scheme 1). In spite of the different structures of polymers 1–3 (cobalt polymer has a chain structure with two carboxylate bridges between the metal atoms,³ the nickel compound exists as a six-membered ring,³ and the structure of the copper polymer can be described as a complex network, in which the dinuclear tetrabridged dimeric fragments are linked to each other *via* a Cu–O interaction with the carboxylate group of the adjacent dinuclear fragment¹⁰), the reactions with N-donors produce the target dinuclear structures in virtually quantitative yields. The reaction of polymer 1 or hexamer 2 ($n = 6$) with quinoline (L^2) in benzene at 80 °C under an inert atmosphere affords the green dinuclear lantern-type complexes $(\text{C}_9\text{H}_7\text{N})_2\text{M}_2(\mu\text{-OOCMe}_3)_4$, where $M = \text{Co}$ (5) or Ni (6), respectively, in yields close to 100% (see Scheme 1). The spectroscopic characteristics of these complexes are very similar to those of the structurally characterized quinoline-containing pivalates.^{1,5}

The reaction of polymer 3 with L^2 in benzene at 80 °C in air produces the green dinuclear complex $(\text{C}_9\text{H}_7\text{N})_2\text{Cu}_2(\mu\text{-OOCMe}_3)_4$ (7) in 89% yield (see Scheme 1).

According to the X-ray diffraction study, the distance between the copper atoms in molecule 7 is 2.6543(9) Å (Fig. 1), this distance being somewhat shorter than the corresponding distances found earlier in the related structurally similar dinuclear cobalt and nickel complexes, $(\text{C}_9\text{H}_7\text{N})_2\text{Co}_2(\mu\text{-OOCMe}_3)_4$ (Co...Co, 2.785 Å)¹ and $(\text{MeC}_9\text{H}_7\text{N})_2\text{Ni}_2(\mu\text{-OOCMe}_3)_4$ (Ni...Ni, 2.754(3) Å),⁵ but longer than those in the dinuclear fragments of the starting polymer 3 (Cu...Cu, 2.580 Å).¹⁰ It should also be



$i. L : M_{\text{at}} = 1 : 1$

noted that the Cu–N distance between the copper atom and the nitrogen atom of the quinoline ligand (2.223(3) Å) is substantially longer than the corresponding distances in the above-mentioned dinuclear cobalt and nickel complexes (Co–N, 2.090 Å; Ni–N, 2.047(9) Å). The N–Cu...Cu–N fragment is virtually linear (N–Cu...Cu angle, 176.32(8)°), unlike the N–Ni...Ni–N fragment characterized by substantial bending (N–Ni...Ni angle, 167.2(4)°).

The investigation of the magnetic properties showed that complexes 5, 6, and 7 exhibit antiferromagnetic spin-spin exchange interactions. The effective magnetic moment μ_{eff} monotonically decreases with decreasing temperature from 5.494 μ_B at 300 K to 0.308 μ_B at 2 K for 5,

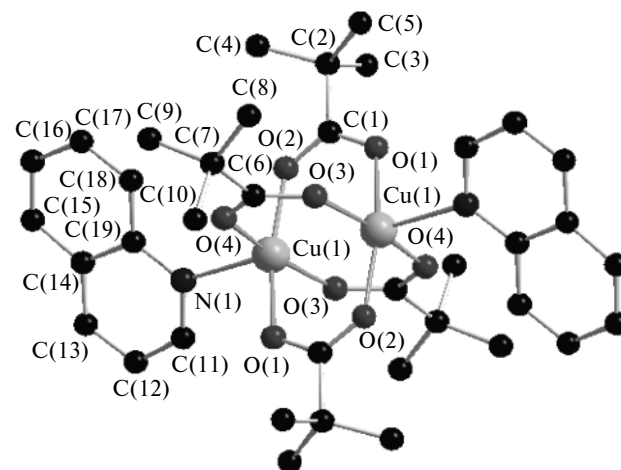


Fig. 1. Structure of the dinuclear complex $(\text{C}_9\text{H}_7\text{N})_2\text{Cu}_2(\mu\text{-OOCMe}_3)_4$ (7).

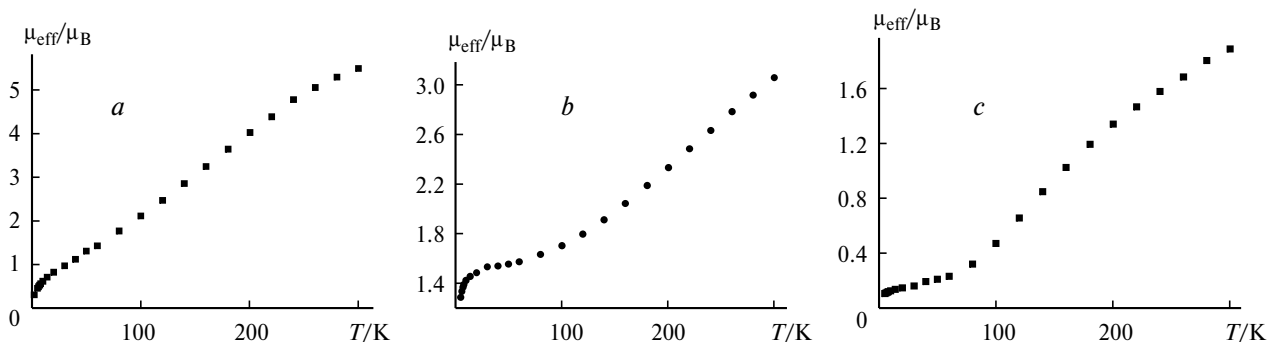


Fig. 2. Magnetic properties of complexes **5** (a), **6** (b), and **7** (c).

from $3.058 \mu_B$ at 300 K to $1.287 \mu_B$ at 5 K for **6**, and from $1.889 \mu_B$ at 300 K to $0.105 \mu_B$ at 5 K for **7** (Fig. 2).

Although we failed to isolate the related complex with Mn^{II} atoms (apparently, due to its very high sensitivity to atmospheric oxygen), we found that the reaction of polymer **4** with L^1 in benzene at 80°C under argon produces the dinuclear complex $(\text{Me}_2\text{C}_5\text{H}_3\text{N})_2\text{Mn}_2(\mu\text{-OOCMe}_3)_4$ (**8**) in 73% yield (see Scheme 1).

According to the X-ray diffraction study, the distances between the metal atoms in molecule **8** are $3.0542(19)$ and $3.0637(13) \text{ \AA}$ (in two independent molecules) (Fig. 3), the observed interatomic distances in **8** being substantially shorter than the corresponding distances found earlier in the structurally similar dinuclear manganese complexes $(\text{C}_{10}\text{H}_9\text{N})_2\text{Mn}_2(\text{OOCCHPh}_2)_4$,¹¹ $(\text{C}_{10}\text{H}_9\text{N})_2\text{Mn}_2(\text{OOCMePh}_2)_4$,¹¹ and $(\text{OC}(\text{CMe}_3)\text{OHNEt}_3)_2\text{Mn}_2(\mu\text{-OOCMe}_3)_4$ (see Ref. 12) ($\text{Mn}\cdots\text{Mn}$, $3.131(2)$, $3.168(4)$, and $3.108(8) \text{ \AA}$, respectively). The $\text{N-Mn}\cdots\text{Mn-N}$ fragment (Mn-N , $2.181(5)$ – $2.184(5) \text{ \AA}$) in molecule **8** is virtually linear ($\text{N-Mn}\cdots\text{Mn-N}$ angle is $173.66(13)$ – $177.93(15)^\circ$). There are short contacts between the hydrogen atoms of the $\alpha\text{-Me}$ substituent in the pyridine ring and the oxygen atoms of the carboxylate groups (2.52 – 2.61 \AA) (see Fig. 3).

Analogous compounds with cobalt (**9**) and nickel (**10**) atoms have been synthesized in our earlier study.³ In the case of the complex with copper atoms, we also used the

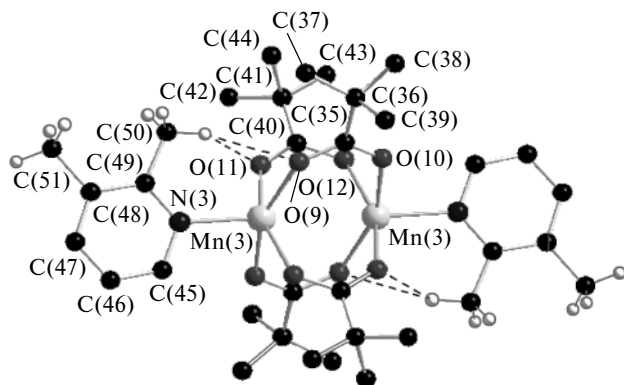


Fig. 3. Structure of complex **8**.

above-described approach. It appeared that the reaction of L^1 ($\text{L} : \text{M}_{\text{at}} = 1 : 1$; 80°C , C_6H_6) with polymeric copper(II) trimethylacetate **3** in air also produced the crystalline complex $(2,3\text{-Me}_2\text{C}_5\text{H}_3\text{N})_2\text{Cu}_2(\mu\text{-OOCMe}_3)_4$ (**11**) (see Scheme 1). The spectroscopic characteristics of this complex are virtually identical to those of the related derivatives of **5** with manganese (**8**), cobalt (**9**), and nickel (**10**) atoms.

The investigation of the magnetic properties showed that complexes **8** and **11**, like analogous tetra-bridged pivalate complexes **9** and **10**,^{3,4} as well as $(\text{MeC}_5\text{H}_3\text{N})_2\text{Cu}_2(\mu\text{-OOCMe}_3)_4$,¹³ exhibit antiferromagnetic spin-spin exchange interactions. The effective magnetic moment μ_{eff} monotonically decreases from $6.615 \mu_B$

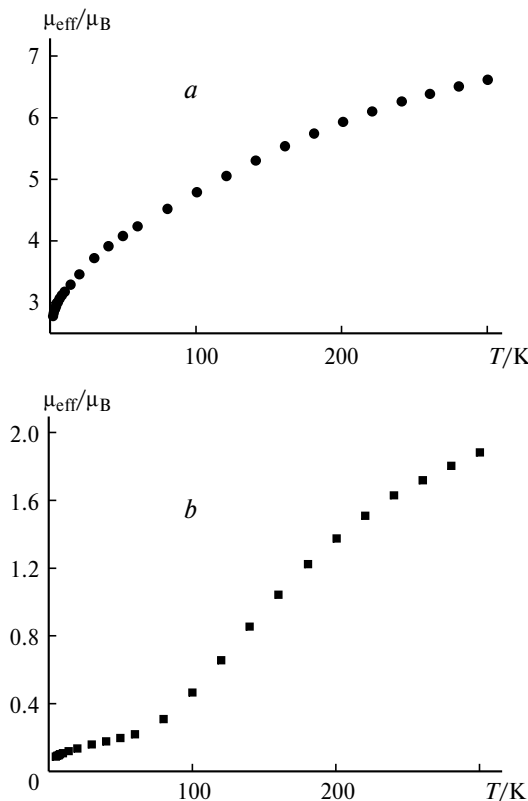


Fig. 4. Magnetic properties of complexes **8** (a) and **11** (b).

at 300 K to $2.781 \mu_B$ at 2 K for **8** and from $1.883 \mu_B$ at 300 K to $0.088 \mu_B$ at 5 K for **11** (Fig. 4).

Therefore, we synthesized series of the dinuclear pivalate complexes with the apical quinoline and 2,3-dimethylpyridine ligands of the composition $(C_9H_7N)_2M_2(\mu-OOCCMe_3)_4$ ($M = Co$ (**5**), Ni (**6**), or Cu (**7**)) and $(Me_2C_5H_3N)_2M_2(\mu-OOCCMe_3)_4$ ($M = Mn$ (**8**), Co (**9**), Ni (**10**), or Cu (**11**)), respectively, as well as the known dinuclear iron complexes. These compounds were used to study the thermolysis.

2. Solid-state thermolysis of dinuclear tetrabridged Mn, Fe, Co, Ni, and Cu pivalates

The solid-state decomposition of the tetrabridged dinuclear pivalate complexes with Mn, Fe, Co, Ni, and Cu atoms proceeds in steps. The following three main steps can be distinguished: the elimination of solvate solvent molecules (if they are present in the crystals), the elimination of neutral *N*-donor ligands, and the degradation of the metal carboxylate core as the major processes. As a rule, the latter step proceeds through the formation of $[M(OOCR)_2]_n$ polymers. However, the compositions of the final thermolysis products substantially depend on the nature of metal atoms and the *N*-donor apical organic ligand.

2.1. Quinoline derivatives

The thermal decomposition of the quinoline complexes $(C_9H_7N)_2M_2(\mu-OOCCMe_3)_4$ ($M = Co$ (**5**), Ni (**6**), or Cu (**7**)) proceeds similarly. For example, the decomposition of cobalt complex **5** starts at 157 ± 2.0 °C (Fig. 5, *a, d*). In the first step (157 – 222 °C), the process is endothermic $\Delta H = 116.5 \pm 8.5$ kJ mol⁻¹, and the weight loss is $33.5 \pm 1.0\%$. Under the experimental conditions, step II is almost not manifested in the thermograms, whereas the weight loss in step III (222 – 300 °C) is $61.7 \pm 1.0\%$.

The total weight loss is $95.2 \pm 1.0\%$. This is not surprising because, as we have demonstrated in the recent study,³ the highly volatile octanuclear complex $Co_8(\mu_4-O)_2(\mu_2-piv)_6(\mu_3-piv)_6$ is the final decomposition product under these conditions, and it is readily removed from the reaction zone.

Nickel complex **6** proved to be thermally more stable (decomposition starts at 231 ± 2 °C; see Fig. 5, *b, e*). In the first step (230 – 280 °C), the process is endothermic, and the weight loss is $33.9 \pm 1.5\%$. The second step (weight loss is $46.8 \pm 1.5\%$) proceeds in the temperature range of 285 – 370 °C and is accompanied by energy release (beginning of the exotherm). In the temperature range of 370 – 450 °C, no weight loss is observed, but the energy is released (exotherm of a complex shape). The total weight

loss is $80.7 \pm 2.0\%$. According to the X-ray powder diffraction analysis, nickel oxide is the final solid decomposition product.

Isostructural copper complex **7** is also thermally stable. The decomposition starts at a temperature above 207 ± 2.0 °C (see Fig. 5, *c, f*). The process proceeds in a rather narrow temperature range from 210 to 310 °C. In this case, two decomposition steps can be distinguished. In step I (210 – 245 °C), melting with decomposition occurs. The melting point is 234.5 ± 1.0 °C. When melting begins, the weight loss is $8.5 \pm 1.0\%$, which is, apparently, indicative of the partial removal of the apical ligand. The end of the melting process (245 ± 2.0 °C; the beginning of the second endotherm) corresponds to the weight loss of $33.1 \pm 1.0\%$. In step II (245 – 310 °C), the process is endothermic (total thermal effect of melting with decomposition is 390.0 ± 9.0 kJ mol⁻¹). The weight loss in the second step is $44.4 \pm 1.5\%$. The total weight loss in the temperature range under investigation is $77.5 \pm 1.5\%$. The composition of the solid decomposition product corresponds to copper(II) oxide (Table 1).

In summary, the decomposition of the dinuclear cobalt, nickel, and copper complexes under study generates either oxides (in the case of nickel and copper) or volatile clusters (in the case of cobalt) (Table 2).

2.2. Dinuclear pivalates with 2,3-dimethylpyridine

The presence of the α -methyl substituent in the pyridine ring leads to substantial changes in the character of thermolysis, although the composition of the final solid product substantially depends on the nature of metal. However, the processes with the involvement of dinuclear structures containing electron-deficient metal atoms, which tend to undergo easy oxidation and are near the middle of the row of the Periodic table (for example, the dimers of manganese and iron $(Me_2C_5H_6N)_2M_2(\mu-OOCCMe_3)_4$, where $M = Mn$ (**8**) or Fe (**12**)),⁷ afford oxides as the final products.

Manganese-containing compound **8** retains thermal stability only below 100 °C (Fig. 6, *a, 7, a*). In the temperature range of 100 – 230 °C, the weight loss in two endothermic steps ($\Delta H = 87.4 \pm 3.0$ kJ mol⁻¹, which is comparable with $\Delta_{vap}H$ for 2,3-dimethylpyridine,¹⁴ two first endotherms) is $30.0 \pm 2.0\%$. In the temperature range of 230 – 470 °C, the weight loss persists, and the processes are accompanied by rather complex energy changes. The total weight loss is $79.3 \pm 2.0\%$. According to the X-ray powder diffraction analysis, Mn_3O_4 is the final solid decomposition product. Unlike the manganese-containing analog, iron compound **12** retains stability in a broader temperature range, up to 160 °C (Figs 6, *e* and 7, *e*). The decomposition starts at 161 – 165 °C. The first step in the temperature range of 165 – 225 °C is endothermic ($\Delta H = 80.5 \pm 2.5$ kJ mol⁻¹, the value is comparable with $\Delta_{vap}H$

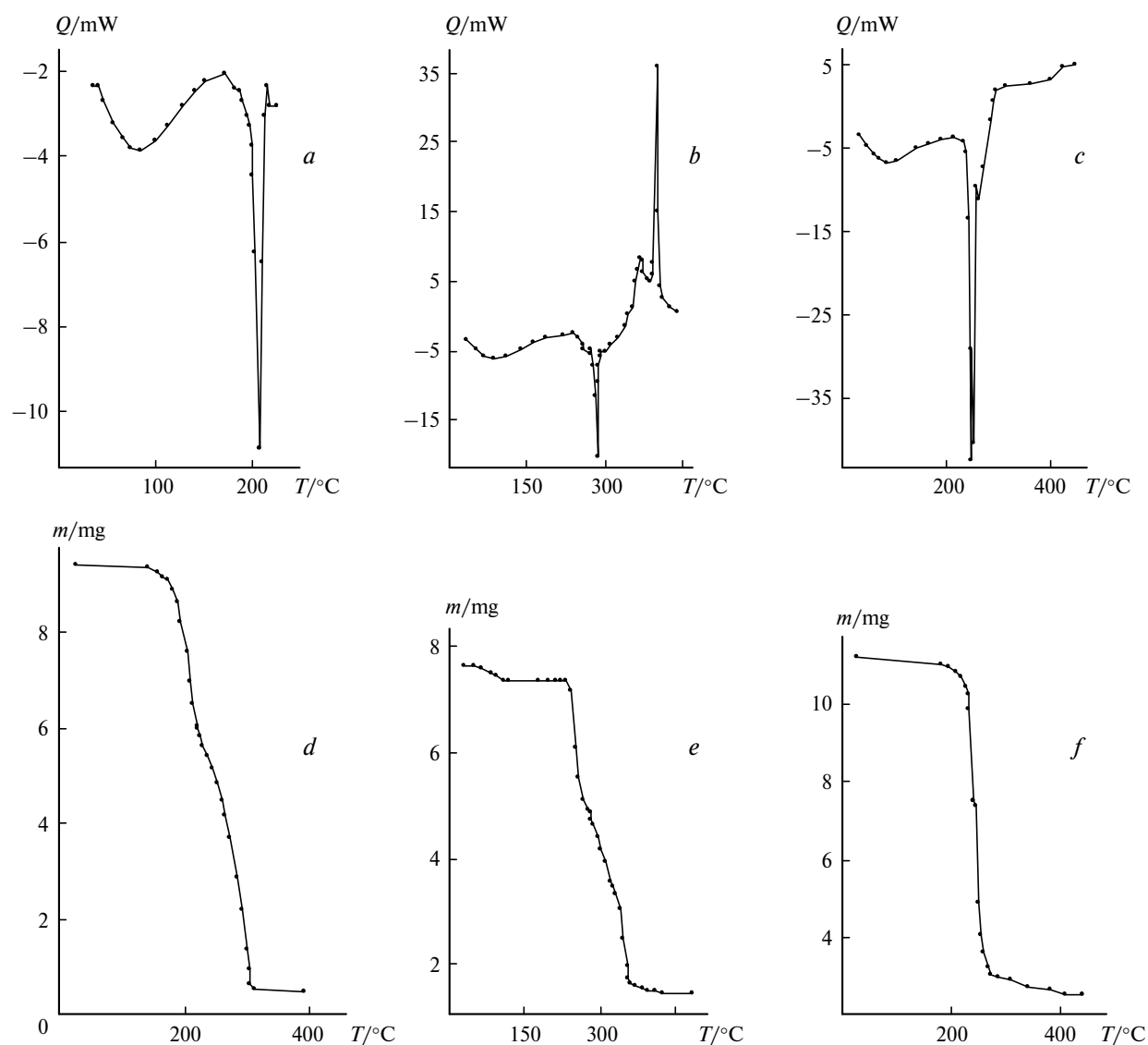


Fig. 5. Temperature dependences of the heat flux (*a–c*) and the weight loss (*d–f*) for complexes **5** (*a, d*), **6** (*b, e*), and **7** (*c, f*).

Table 1. X-ray powder diffraction analysis of solid decomposition products of compounds **7** and **11**

Decomposition product of 7		Decomposition product of 11		CuO [48–1548]*		Cu ₂ O [5–667]*		Cu [4–836]*	
<i>d</i> /Å	<i>I</i> / <i>I</i> ₀ (%)	<i>d</i> /Å	<i>I</i> / <i>I</i> ₀ (%)	<i>d</i> /Å	<i>I</i> / <i>I</i> ₀ (%)	<i>d</i> /Å	<i>I</i> / <i>I</i> ₀ (%)	<i>d</i> /Å	<i>I</i> / <i>I</i> ₀ (%)
2.535	30	2.530	20	2.532	37				
2.530	100	2.520	100	2.524	100				
		2.465	20			2.465	100		
2.330	80	2.330	80	2.324	99				
		2.135	5			2.135	37		
		2.090	40					2.088	100
1.860	10	1.855	10	1.868	30				
1.505	10	1.505	10	1.506	20	1.510	27		
1.375	10	1.375	10	1.375	14				
		1.278	20					1.278	80

* Powder Diffraction File, Swarthmore: Joint Committee on Powder Diffraction Standards.

Table 2. Characteristics of the decomposition of the dinuclear tetrabridged cobalt complexes

Characteristics	5	6	7
Boiling point of the ligand/°C	238	238	238
Number of steps	2	2	2
Temperature of the onset of decomposition/°C	157	231	207
Temperature range of step I/°C	157–222	231–280	207–245
Temperature range of step II/°C	*	**	245–310
Temperature range of step III/°C	222–300	285–370	—
Temperature of cessation of decomposition/°C	300	450	320
Final decomposition product	Co ₈ (O) ₂ (piv) ₁₂	NiO	CuO

* Was not isolated.

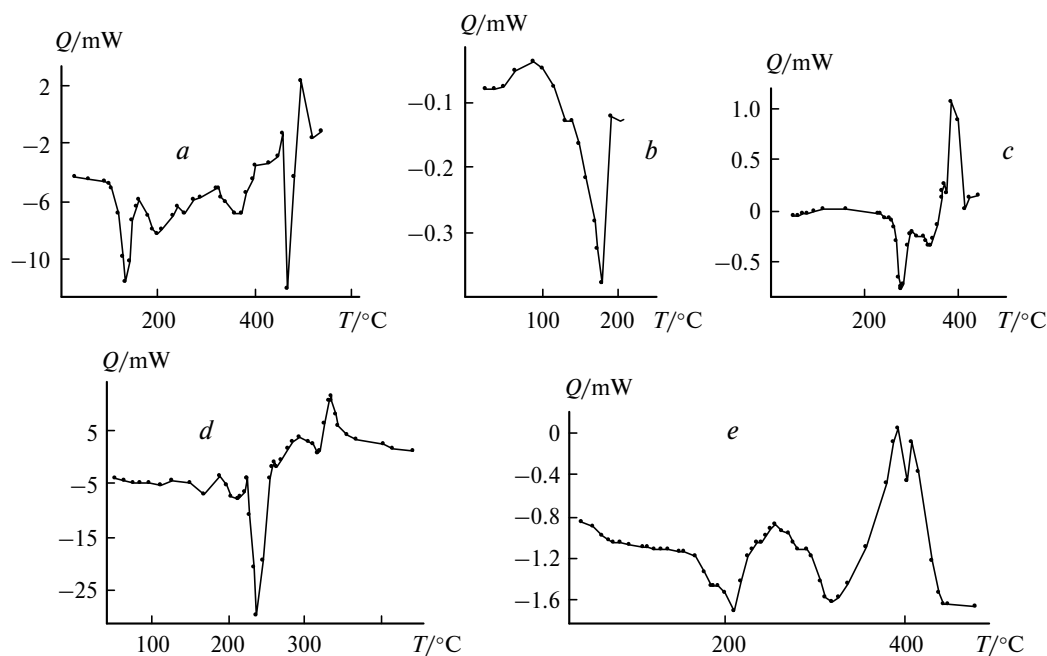
** Was not virtually isolated.

for 2,3-dimethylpyridine¹⁴), and the weight loss in this step is $30.3 \pm 1.5\%$ (theoretical percentage of 2,3-dimethylpyridine in the complex is 29.3%). Presumably, the process proceeding in this temperature range corresponds to the removal of the coordinated ligand. In the temperature range of 225–275 °C, no weight loss is observed, but the energy is released, which is generally characteristic of the formation of a new structure. The further heating in the temperature range of 275–440 °C leads to the further weight loss ($48.5 \pm 1.5\%$) accompanied by complex energy transformations in the sample. The energy changes qualitatively correspond to those observed earlier in the course of thermal decomposition of the $[\text{Fe}(\mu\text{-OOCMe}_3)_2]_n$ polymer at temperatures above 280 °C.¹⁵ This suggests that the polymeric iron pivalate complex is formed in the temperature range of 225–275 °C, and then this complex is decomposed. The total weight loss is $78.8 \pm 2.0\%$, and

$\alpha\text{-Fe}_2\text{O}_3$ is the final decomposition product (X-ray powder diffraction data).

The decomposition of the cobalt complex $(2,3\text{-Me}_2\text{C}_5\text{H}_3\text{N})_2\text{Co}_2(\text{OOC-Bu}^t)_4$ (**9**) starts already at 97 ± 2 °C (see Figs 6, *b* and 7, *b*). In the first step (97–170 °C), the processes are endothermic ($\Delta H = 89.5 \pm 5.0$ kJ mol⁻¹), and the weight loss is $29.8 \pm 1.0\%$, which corresponds to elimination of both 2,3-dimethylpyridine molecules. Neither the weight loss nor changes in the heat flux are observed in step II (170–210 °C). In step III (220–280 °C), the weight loss is $65.0 \pm 1.0\%$. The total weight loss is $94.8 \pm 1.0\%$, which corresponds primarily to the formation of the volatile cluster $\text{Co}_8(\mu_4\text{-O})_2(\mu_2\text{-piv})_6(\mu_3\text{-piv})_6$.

The nickel complex $(2,3\text{-Me}_2\text{C}_5\text{H}_3\text{N})_2\text{Ni}_2(\text{OOC-Bu}^t)_4$ (**10**) is thermally stable, and its decomposition starts at temperatures above 225 °C (see Figs 6, *c* and 7, *c*). Two

**Fig. 6.** Temperature dependences of the heat flux change for complexes **8** (*a*), **9** (*b*), **10** (*c*), **11** (*d*), and **12** (*e*).

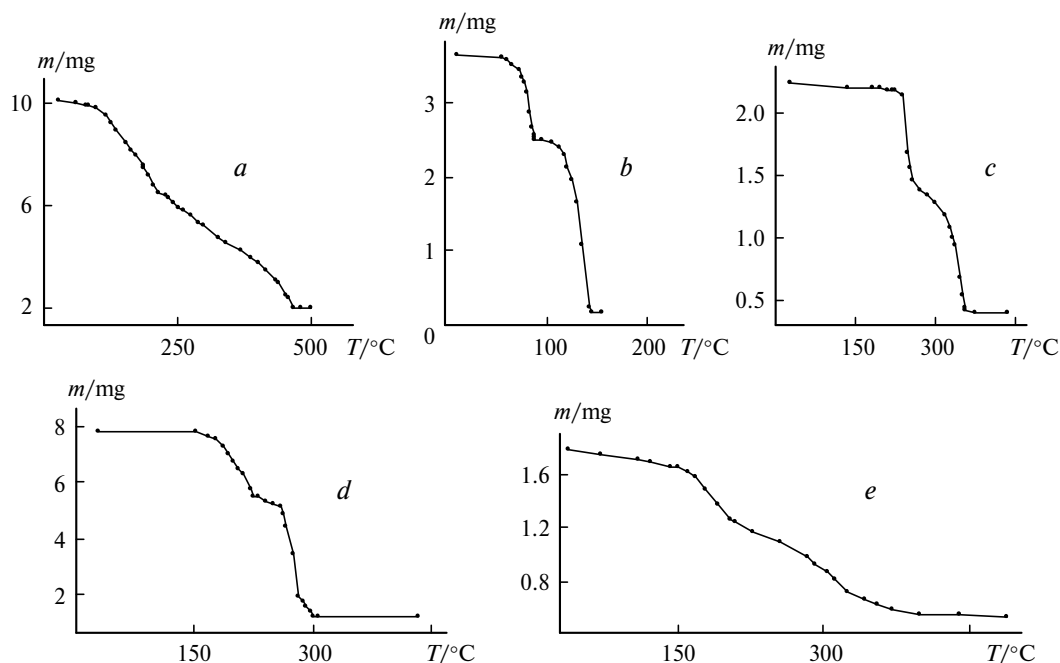


Fig. 7. Temperature dependences of the weight loss for complexes **8** (a), **9** (b), **10** (c), **11** (d), and **12** (e).

steps are clearly distinguished. The weight loss in the first step is $38.0 \pm 2.0\%$, which is substantially larger than the theoretical percentage of 2,3-dimethylpyridine in the complex (28.9%) and is, apparently, indicative of intramolecular reactions proceeding with the involvement of carboxylate groups. The process is endothermic. At temperatures above 280 $^{\circ}\text{C}$, the process is exothermic. The total weight loss in the overall temperature range is $84.0 \pm 2.0\%$. According to the X-ray powder diffraction analysis, nickel metal is the final decomposition product. This result is quite unexpected because the earlier study¹⁶ has demonstrated that the thermolysis of dinuclear nickel complexes containing the structurally similar tetrabridged metal carboxylate core with the apical pyridine¹⁶ and quinoline ligands affords NiO. Apparently, this is due to the influence of the methyl group in the α position acting as an intramolecular reducing agent and promoting intramolecular ligand-ligand redox reactions already in the first step of decomposition.

Several steps are clearly distinguished in the thermal decomposition process of the copper complex $(2,3\text{-Me}_2\text{C}_5\text{H}_3\text{N})_2\text{Cu}_2(\mu\text{-OOCMe}_3)_4$ (**11**) (see Figs 6, *d* and 7, *d*). In the first step, in the temperature range of 153–230 $^{\circ}\text{C}$ (± 2 $^{\circ}\text{C}$), the total weight loss is $30.0 \pm 1.0\%$, which is also slightly larger than the theoretical percentage of 2,3-dimethylpyridine in the molecule. This step includes, in turn, the following two steps: the step in the temperature range of 153–188 $^{\circ}\text{C}$ with the weight loss of $14.3 \pm 1.0\%$ and the step in the temperature range of 188–230 $^{\circ}\text{C}$ with the weight loss of $15.7 \pm 1.0\%$. Both steps are accompanied by energy absorption (endotherms),

which does not exclude intramolecular interactions. Step II (230–260 $^{\circ}\text{C}$ (± 2 $^{\circ}\text{C}$)) is accompanied by a small weight loss but by a rather large endotherm (266.7 ± 9.5 kJ mol⁻¹), which apparently corresponds to the structural rearrangement of the compound. Finally, in step III (260–320 $^{\circ}\text{C}$), the weight loss is $50.2 \pm 1.5\%$, the processes are exothermic, and the energy changes are rather complex. The total weight loss in the temperature range under study is $80.0 \pm 1.5\%$. The phase composition of the final solid decomposition product determined by X-ray powder diffraction (see Table 1) is rather complex and corresponds to a mixture of the CuO, Cu₂O, and Cu phases. A comparison of the intensities of the main reflections for the phases and the results of the thermogravimetric analysis suggest that the phases are present in a ratio of 4 : 1 : 2.

The decomposition of dinuclear pivalate complexes of 3d metals, from manganese to copper, with 2,3-dimethylpyridine ligands showed that active hydrocarbon substituents in the α position can substantially influence the character of the thermolysis products, particularly, in the case of the thermal degradation of complexes with metals at the end of the row of the Periodic table having a rather high oxidation potential (Table 3).

To summarize, we found possible ways of varying mild thermolysis products of the whole class of coordination precursors, in particular, of dinuclear tetrabridged pivalate dimers with Group VII and VIII 3d metals and copper. In our opinion, this result opens possibilities for the preparation of various films and coatings based on this class of carboxylates, whose synthesis presents no difficulties.

Table 3. Characteristics of the decomposition of the dinuclear tetrabridged complexes with 2,3-dimethylpyridine

Characteristics	8	12	9	10	11
Boiling point of the ligand/°C	163.7	163.7	163.7	163.7	163.7
Number of steps	3	3	3	2	3
Temperature of the onset of decomposition/°C	100	161–165	97	229	153
Temperature range of step I/°C	100–230	165–225	97–170	230–280	153–230
Temperature range of step II/°C	265–290	275–300	170–210	280–380	230–260
Temperature range of step III/°C	290–380	300–380	220–280	*	260–320
Temperature of cessation of decomposition/°C	420	420	280	420	400
Final decomposition product	Mn ₃ O ₄	Fe ₂ O ₃	Co ₈ (O) ₂ (piv) ₁₂	Ni	CuO, Cu ₂ O, Cu

* The steps of melting of the complex, the removal of the coordinated ligand, and the complete degradation of the metal core were not distinguished in the temperature dependence of the weight loss.

Experimental

All synthetic operations were carried out under pure argon with the use of oxygen-free or anhydrous solvents using the standard Schlenk technique. The starting polynuclear pivalates [M(OOCBu^t)₂]_n (M = Co,³ Ni,³ or Cu¹⁷), [(η¹-EtOH)Mn(μ-OOCCMe₃)₂]_n,¹⁸ and (Me₂C₅H₃N)₂M₂(μ-OOCCMe₃)₄ (M = Co,³ Ni,³ or Fe⁷) were prepared according to procedures described earlier. The synthesis of new compounds was carried out with the use of trimethylacetic acid (Acros Organics), 2,3-dimethylpyridine (Acros Organics), and quinoline (Aldrich).

The IR spectra of compounds **5–11** were recorded on a Specord M-80 spectrophotometer in KBr pellets. The elemental analysis of compounds **5–11** was carried out on a Carlo Erba C,H,N analyzer in the Center of Collaborative Research of the N. S. Kurnakov Institute of General and Inorganic Chemistry of the Russian Academy of Sciences. The static magnetic susceptibility was measured on a SQUID MPMS-59 Quantum Design magnetometer in the temperature range of 2–300 K. The effective magnetic moments were calculated by the equation $\mu_{\text{eff}} = (8\chi_{\text{M}}T)^{1/2}$.

The thermal decomposition of compounds **5–12** was studied by differential scanning calorimetry and thermogravimetry on DSC-20 and TG-50 units of a Mettler TA-3000 thermoanalyzer. Samples of compounds **5–12** were heated under dry argon at a constant rate of 5 deg min⁻¹ (in all experiments). For each compound, two differential scanning calorimetry experiments and three thermogravimetric experiments were performed. The weight loss upon thermal degradation was determined directly on the TG-50 unit; the accuracy of weighing was $\pm 2 \cdot 10^{-3}$ mg. The thermal decomposition was studied in steps by differential scanning calorimetry, which involved the division of the total temperature range into intervals. The size and number of these intervals were determined based on the overall pattern of the weight loss upon decomposition. This approach allowed us to determine the weight loss in each temperature range and compare the results of DSC with the thermogravimetric data. The results of these methods were in satisfactory agreement, which confirms the reliability of the experimental data. The accuracy of the determination of anomalous points and thermal effects in the DSC curves was $\pm 1^\circ$ and $\pm 0.5\%$, respectively.

The X-ray powder diffraction analysis of the decomposition products was carried out on a FR-552 monochromator chamber

(CuK_{α1} radiation) using germanium as the internal standard (X-ray diffraction patterns were processed on an IZA-2 comparator with an accuracy of ± 0.01 mm) and with the use of the STOE Powder Diffraction System.

Synthesis of complexes

Bis(quinolino)tetra(μ₂-O,O'-trimethylacetato)dicobalt(II), (C₉H₇N)₂Co₂(μ₂-OOCCMe₃)₄ (5**).** A solution of quinoline (0.198 g, 1.53 mmol) in benzene (30 mL) was added to [Co(OOCCMe₃)₂]_n (0.4 g, 1.53 mmol; per formula unit Co(OOCCMe₃)₂). The solution was stirred at 80 °C for 20 min. The resulting red-crimson-colored solution was concentrated at 0.1 Torr and 20 °C to 15 mL and allowed to crystallize at 5 °C. Green crystals that precipitated after storage for 24 h were separated by decantation, washed with benzene, and dried under a stream of argon. The yield of compound **5** was 0.57 g (95.0% based on the starting amount of the ligand). Found (%): C, 58.02; H, 6.58; N, 3.38. Co₂C₃₈H₅₀N₂O₈. Calculated (%): C, 58.48; H, 6.41; N, 3.6. IR (KBr), ν/cm⁻¹: 3272 w, 2960 w, 2364 w, 2344 m, 2324 w, 1700 w, 1684 w, 1668 w, 1610 v.s, 1512 m, 1480 s, 1456 m, 1420 v.s, 1372 m, 1356 m, 1224 m, 1052 s, 956 w, 892 m, 804 s, 784 s, 736 w, 608 s, 488 w, 420 w, 324 w.

The synthesis afforded crystals suitable for X-ray diffraction.

Bis(quinolino)tetra(μ₂-O,O'-trimethylacetato)dinickel(II), (C₉H₇N)₂Ni₂(μ₂-OOCCMe₃)₄ (6**).** A solution of quinoline (0.148 g, 1.15 mmol) in benzene (25 mL) was added to Ni₆(OOCCMe₃)₁₂ (0.3 g, 0.15 mmol). The pale-green reaction solution was stirred at 80 °C for 20 min, concentrated at 0.1 Torr and 20 °C to 10 mL, and allowed to crystallize at 20 °C. Dark-green crystals that precipitated after storage for 24 h were separated by decantation, washed with cold benzene, and dried under a stream of argon. The yield of compound **6** was 0.39 g (87% based on the starting amount of the ligand). Found (%): C, 58.12; H, 6.90; N, 3.83. Ni₂C₃₈H₅₀O₈N₂. Calculated (%): C, 58.5; H, 6.4; N, 3.6. IR (KBr), ν/cm⁻¹: 3226 w, 2956 w, 2924 w, 1772 w, 1684 w, 1614 w, 1595 v.s, 1484 s, 1456 m, 1420 v.s, 1376 m, 1360 m, 1224 m, 1052 s, 960 w, 896 m, 800 s, 780 s, 736 w, 616 s, 492 w, 432 m.

The synthesis afforded crystals suitable for X-ray diffraction.

Bis(quinolino)tetra(μ₂-O,O'-trimethylacetato)dicopper(II), (C₉H₇N)Cu₂(μ₂-OOCCMe₃)₄ (7**).** Quinoline (0.146 g, 1.13 mmol) was added to a solution of [Cu₂(OOCCMe₃)₄]_n (0.3 g, 1.13 mmol; per formula unit Cu(OOCCMe₃)₂) in ben-

Table 4. Crystallographic parameters of complexes **7** and **8**

Parameter	7	8
Molecular formula	C ₃₈ H ₅₀ Cu ₂ N ₂ O ₈	C ₃₄ H ₅₄ Mn ₂ N ₂ O ₈
Molecular weight	789.88	728.67
Space group	<i>P2</i> (1)/ <i>c</i>	<i>P2</i> (1)/ <i>c</i>
<i>a</i> /Å	11.7401(10)	11.096(3)
<i>b</i> /Å	18.7762(10)	18.743(5)
<i>c</i> /Å	9.3483(10)	32.408(8)
α/deg	90	90
β/deg	96.669(10)	91.373(10)
γ/deg	90	90
<i>V</i> /Å ³	2046.7(3)	6738(3)
<i>Z</i>	2	6
ρ _{calc} /g cm ⁻³	1.282	1.077
μ/cm ⁻¹	1.677	0.602
Radiation	Cu-Kα (λ = 1.5418 Å)	Mo-Kα (λ = 0.71073 Å)
θ-2θ-Scan range/deg	3.79–74.90	1.66–25.03
Number of measured reflections	4280	26592
Number of reflections with <i>I</i> > 2σ(<i>I</i>)	4034	10075
<i>R</i> ₁	0.0614	0.0908
<i>wR</i> ₂	0.1884	0.2168

zene (30 mL). The reaction solution was stirred at 80 °C for 15 min, concentrated at 0.1 Torr and 20 °C to 15 mL, and allowed to crystallize at 20 °C. Green crystals that precipitated after storage for 24 h were separated by decantation, washed with cold benzene, and dried in air. The yield of compound **7** was 0.4 g (89.7% based on the starting amount of copper). Found (%): C, 57.82; H, 6.48; N, 3.31. C₃₈H₅₀Cu₂N₂O₈. Calculated (%): C, 57.72; H, 6.33; N, 3.54. IR (KBr), ν/cm⁻¹: 3232 m, 2960 w, 1664 w, 1508 m, 1480 m, 1416 m, 1360 w, 1316 w, 1260 w, 1044 s, 952 w, 896 w, 816 w, 804 s, 780 s, 736 w, 616 s, 488 w, 440 m.

The synthesis afforded crystals suitable for X-ray diffraction.

Bis(2,3-dimethylpyridino)tetra(μ₂-*O*,*O'*-trimethylacetato)dimanganese(II), (2,3-(CH₃)₂C₅H₃N)₂Mn₂(μ₂-OOCMe₃)₄ (8**).** A solution of 2,3-dimethylpyridine (0.16 g, 1.5 mmol) in benzene (20 mL) was added to [(η¹-EtOH)Mn(μ-OOCMe₃)₂]_n (0.3 g, 1.0 mmol). The reaction mixture was stirred at 80 °C under argon for 1 h. The resulting solution was filtered, concentrated to 8 mL, and kept at 20 °C for 3 days. Colorless crystals that precipitated were separated from the solution by decantation, washed with cold benzene (10 °C), and dried under a stream of argon. The yield of compound **8** was 0.27 g (73% based on the starting amount of manganese). Found (%): C, 56.3; H, 7.6; N, 4.0. C₃₄H₅₄Mn₂N₂O₈. Calculated (%): C, 56.04; H, 7.47; N, 3.84. IR (KBr), ν/cm⁻¹: 2956 m, 2928 m, 2872 w, 1664 m, 1612 s, 1480 m, 1456 w, 1420 s, 1372 m, 1360 m, 1284 w, 1260 w, 1228 m, 1192 w, 1140 w, 1140 w, 1100 w, 1016 m, 936 w, 892 m, 856 w, 812 m, 788 m, 748 w, 724 w, 672 w, 604 s, 572 w, 416 s.

The synthesis afforded crystals suitable for X-ray diffraction.

Bis(2,3-dimethylpyridino)tetra(μ₂-*O*,*O'*-trimethylacetato)dicopper(II), (CH₃)₂C₅H₃N)₂Cu₂(μ₂-OOCMe₃)₄ (11**).** 2,3-Dimethylpyridine (0.202 g, 1.88 mmol) was added to a solution of [Cu₂(OOCMe₃)₄]_n (0.5 g, 1.88 mmol; per formula unit Cu(OOCMe₃)₂) in benzene (30 mL). The reaction mixture was stirred at 80 °C for 5 min, concentrated at 0.1 Torr and

20 °C to 15 mL, and allowed to crystallize at ~20 °C. Dark-green crystals that precipitated after storage for 24 h were separated by decantation, washed with cold benzene, and dried in air. The yield of compound **11** was 0.404 g (80.8% based on the starting amount of copper). Found (%): C, 54.83; H, 7.95; N, 3.37. C₃₄H₅₄Cu₂N₂O₈. Calculated (%): C, 54.69; H, 7.24; N, 3.75. IR (KBr), ν/cm⁻¹: 3852 w, 3428 w, 2960 m, 2456 w, 2328 m, 2064 w, 1732 w, 1612 v. s, 1480 s, 1372 s, 1224 m, 896 s, 788 w, 724 w, 624 w, 436 w, 356 w, 320 s.

The synthesis afforded crystals suitable for X-ray diffraction.

X-ray diffraction study. X-ray reflections for complex **7** were measured on an automated Enraf-Nonius CAD-4 diffractometer; for complex **8**, on an automated Bruker AXS SMART 1000 diffractometer equipped with a CCD detector (graphite monochromator, 120 K, ω-scanning technique, the scan step was 0.3°, the exposure time per frame was 30 s) using a standard procedure.¹⁹ Semiempirical absorption corrections were applied.²⁰ The crystallographic parameters and the refinement statistics for the structures of **7** and **8** are given in Table 4.

The structures of both complexes were solved by direct methods and refined by the full-matrix least-squares method with anisotropic displacement parameters for all nonhydrogen atoms (except for the methyl carbon atoms of the disordered *tert*-butyl groups, which were refined isotropically). The hydrogen atoms of the *tert*-butyl substituents of the pivalate ligands and the pyridine rings in the coordinated amine molecules were positioned geometrically and refined using a riding model. All calculations were performed with the use of the SHELX97 program package.²¹

This study was financially supported by the Russian Foundation for Basic Research (Project Nos 07-03-00408, 07-03-00707, 05-03-32767, 05-03-794, 05-03-08203, and 06-03-08086), the Russian Academy of Sciences (Target Program for Basic Research of the Division of Chemistry

and Materials Science of the Russian Academy of Sciences "Chemistry and Physical Chemistry of Supramolecular Systems and Atomic Clusters" and the Programs of the Presidium of the Russian Academy of Sciences "Molecular Design of Magnetoactive Compounds and Materials (Molecular Magnets)" and "Polyfunctional Materials for Molecular Electronics"), the Council on Grants of the President of the Russian Federation (Program for State Support of Leading Scientific Schools of the Russian Federation, Grant NSh 4959.2006.03), and the Federal Agency for Science and Innovations of the Russian Federation (Program "Nanotechnologies and Nanomaterials").

References

1. Y. Cui, D.-L. Long, X.-Y. Huang, F.-K. Zheng, W.-D.-Chen, and J.-S. Huang, *Chinese J. Struct. Chem.*, 1999, **18**, p.9; 107.
2. E. V. Pakhmutova, A. E. Malkov, T. B. Mikhailova, A. A. Sidorov, I. G. Fomina, G. G. Aleksandrov, V. M. Novotortsev, V. N. Ikorskii, and I. L. Eremenko, *Izv. Akad. Nauk, Ser. Khim.*, 2003, 2006 [*Russ. Chem. Bull.*, 2003, **52**, 2105 (Engl. Transl.)].
3. I. G. Fomina, G. G. Aleksandrov, Zh. V. Dobrokhotova, O. Yu. Proshenkina, M. A. Kiskin, Yu. A. Velikodnyi, V. N. Ikorskii, V. M. Novotortsev, and I. L. Eremenko, *Izv. Akad. Nauk, Ser. Khim.*, 2006, 1841 [*Russ. Chem. Bull., Int. Ed.*, 2006, **55**, 1909].
4. I. L. Eremenko, S. E. Nefedov, A. A. Sidorov, and I. I. Moiseev, *Izv. Akad. Nauk, Ser. Khim.*, 1999, 409 [*Russ. Chem. Bull.*, 1999, **48**, 405 (Engl. Transl.)].
5. N. I. Kirilova, Yu. T. Struchkov, M. A. Porai-Koshits, A. A. Pasynskii, A. S. Antsyshkina, L. Kh. Minacheva, G. G. Sadikov, T. Ch. Idrisov, and V. T. Kalinnikov, *Inorg. Chim. Acta*, 1980, **42**, 115.
6. M. A. Kiskin and I. L. Eremenko, *Usp. Khim.*, 2006, **7**, 627 [*Russ. Chem. Rev.*, 2006, **7**, 559 (Engl. Transl.)].
7. A. A. Sidorov, I. G. Fomina, G. G. Aleksandrov, Yu. V. Rakitin, V. M. Novotortsev, V. N. Ikorskii, M. A. Kiskin, and I. L. Eremenko, *Izv. Akad. Nauk, Ser. Khim.*, 2004, 460 [*Russ. Chem. Bull., Int. Ed.*, 2004, **53**, 483].
8. V. M. Novotortsev, Yu. V. Rakitin, S. E. Nefedov, and I. L. Eremenko, *Izv. Akad. Nauk, Ser. Khim.*, 2000, 437 [*Russ. Chem. Bull., Int. Ed.*, 2000, **49**, 438].
9. Y. V. Rakitin, V. M. Novotortsev, V. N. Ikorskii, and I. L. Eremenko, *Mendeleev Commun.*, 2006, 23.
10. E. G. Il'ina, S. I. Troyanov, and K. M. Dunaeva, *Koord. Khim.*, 1992, **18**, 882 [*Russ. J. Coord. Chem.*, 1992, **18**, 882 (Engl. Transl.)].
11. E. V. Amel'chenkova, T. O. Denisova, and S. E. Nefedov, *Mendeleev Commun.*, 2004, 103.
12. Y. Zhang, L. Jianmin, Z. Min, Q. Wang, and X. Wu, *Chem. Lett.*, 1998, 1051.
13. Yu. V. Rakitin and V. T. Kalinnikov, *Sovremennaya magneto-khimiya [Modern Magnetochemistry]*, Nauka, St. Petersburg, 1994, (in Russian).
14. V. Majer and V. Svoboda, *Enthalpies of Vaporization of Organic Compounds: A Critical Review and Data Compilation*, Blackwell Scientific Publications, Oxford, 1985, 300.
15. M. A. Kiskin, G. G. Aleksandrov, Zh. V. Dobrokhotova, V. M. Novotortsev, Yu. G. Shvedenkov, and I. L. Eremenko, *Izv. Akad. Nauk, Ser. Khim.*, 2006, 779 [*Russ. Chem. Bull., Int. Ed.*, 2006, **55**, 806].
16. Zh. V. Dobrokhotova, I. G. Fomina, M. A. Kiskin, A. A. Sidorov, V. M. Novotortsev, and I. L. Eremenko, *Izv. Akad. Nauk, Ser. Khim.*, 2006, 250 [*Russ. Chem. Bull., Int. Ed.*, 2006, **55**, 256].
17. T. O. Denisova, E. V. Amel'chenkova, I. V. Pruss, Zh. V. Dobrokhotova, O. P. Fialkovskii, and S. E. Nefedov, *Zh. Neorg. Khim.*, 2006, **7**, 1098 [*Russ. J. Inorg. Chem.*, 2006, **7**, 1020 (Engl. Transl.)].
18. M. A. Kiskin, I. G. Fomina, G. G. Aleksandrov, A. A. Sidorov, V. M. Novotortsev, Y. V. Rakitin, Z. V. Dobrokhotova, V. N. Ikorskii, Y. G. Shvedenkov, I. L. Eremenko, and I. I. Moiseev, *Inorg. Chem. Commun.*, 2005, **8**, 89.
19. *SMART (Control) and SAINT (Integration) Software, Version 5.0*, Bruker AXS Inc., Madison, WI, 1997.
20. G. M. Sheldrick, *SADABS, Program for Scanning and Correction of Area Detector Data*, Göttingen University, Göttingen, Germany, 1997.
21. G. M. Sheldrick, *SHELX97, Program for the Solution of Crystal Structures*, Göttingen University, Göttingen, Germany, 1997.

Received February 1, 2007;
in revised form April 25, 2007